AIAA-98-1955

NONLINEAR AEROELASTIC ANALYSIS OF AIRCRAFT WITH HIGH-ASPECT-RATIO WINGS

Mayuresh J. Patil[*], **Dewey H. Hodges**[†]
Georgia Institute of Technology, Atlanta, Georgia
and
Carlos E. S. Cesnik[‡]
Massachusetts Institute of Technology, Cambridge, Massachusetts

Abstract

The paper describes a formulation for aeroelastic analysis of aircraft with high-aspect-ratio wings. The analysis is a combination of a geometrically-exact mixed formulation for dynamics of moving beams and finite-state unsteady aerodynamics with the ability to model dynamic stall. The analysis also takes into account gravitational forces, propulsive forces and rigid-body dynamics. The code has been validated against the exact flutter speed of the "Goland" wing. Further results have been obtained which give insight into the effects of the structural and aerodynamic nonlinearities on the trim solution and flutter speed.

Introduction

High-aspect-ratio wings have come into prominence lately due to the interest in High Altitude Long Endurance (HALE) aircrafts for future military as well as civilian missions. Military missions include, *i)* reconnaissance: requirements are of long range and substantial loiter period to be able to gather required information and to help in targeting, *ii)* massive airlifter: the "million pound" airlifter is required to have a long range ($\sim 12,000$ NM), capable of returning to base after cargo delivery. HALE aircraft have to have very high lift-to-drag ratio wings, thus leading to high aspect ratios.[1]

The Uninhabited Reconnaissance Aerial Vehicle (URAV) will be essentially autonomous with as few manual inputs as possible.[2] These would require an accurate model which is also amenable to control design.[3] Also, in the future there is a possibility of Uninhabited Combat Aerial Vehicles (UCAV) that will push for high maneuverability, extending the flight envelope into higher angles of attack.

Long wings tend to have large deflections. Thus, an accurate modeling of non-linear phenomena in aeroelasticity would be very much a part of next generation aircraft design. Such a model would also be required in designing a control system for the entire expected flight regime. This paper presents the ongoing research toward development of such a model. High-fidelity computational techniques are already available for both the structural analysis and aerodynamics,[4] but the emphasis in this research is towards using a far less computationally expensive model. The reasons lie in the goals of this exercise, viz., *i)* to develop an inexpensive but reasonably high fidelity model which might help get more insight into the true nonlinear aeroelastic behavior and its control, *ii)* to build an analysis tool for preliminary design and control system design.

Background

Aeroelastic analysis of composite wings is a subject of an ever increasing body of literature. The

[*]Graduate Research Assistant, School of Aerospace Engineering. Member, AIAA.

[†]Professor, School of Aerospace Engineering. Fellow, AIAA. Member, AHS.

[‡]Boeing Assistant Professor of Aeronautics and Astronautics. Senior Member, AIAA. Member, AHS.

interest stems from the possibility of using directional properties of composites to optimize a wing (i.e., aeroelastic tailoring). Ref. 5 presents a historical background of aeroelastic tailoring and the theory underlying the technology. The paper provides historical perspective on the development of codes and the activities of various research groups up to that time. It is still true that in many studies, the structural deformation model used is that a beam-like wing, since tailoring focuses on bend-twist deformation coupling. Restraining the freedom of the chordwise bending mode, which is often done, can result in substantially different natural frequencies and mode shapes for highly coupled laminates. Also, the prudence of retaining rigid-body modes in flutter analysis during design iterations was pointed out.

In Ref. 6, static aeroelastic problems such as spanwise lift redistribution, lift effectiveness, and aileron effectiveness are discussed. Two theoretical models are commonly used: (1) laminated plate theory with elementary strip theory airloads and (2) a more general representation of the laminated wing structure, in matrix form, with discrete-element aerodynamics. In the latter case the box beam is characterized by bending stiffness EI, torsional stiffness GJ, and bending-twist coupling K. These are derived from classical plate theory applied to the top and bottom flanges.

While it is true that some high-fidelity models exist,[4] in the present research effort the use of beam models is emphasized. When the aspect ratio is sufficiently high, the main concern ceases to be the plate-like deformation and turns instead to geometrically nonlinear beam-like behavior. In this case it is also important to accurately characterize the "equivalent beam" properties of the wing. There are two philosophies concerning this. One is to assume a simplified geometry, such as a box beam. Librescu and his co-workers were among the first to use a box beam model made up of various composite laminates for the wing[7, 8] – as opposed to laminated plates. This type of model was analyzed for static aeroelastic instabilities. The focus was on potentially advantageous use of bending-torsion structural coupling. Higher-order effects such as transverse shear flexibility and warping restraint were also considered.

Aeroelastic characteristics of highly flexible aircraft is investigated by van Schoor and von Flotow.[9] The complete aircraft was modeled using a few modes of vibration, including rigid-body modes. Banerjee and his co-workers have been working on a similar problem and have investigated the optimization of a composite cantilevered beam with frequency and aeroelastic constraints.[10, 11] The dynamic stiffness matrix method is used for modal analysis of the beam. In another study, parametric analysis of box beams with thick walls is being conducted by Chattopadhyay and co-workers.[12] Here, higher-order laminate theory is used for each wall of the box beam. The authors of the present paper have also investigated the influence of ply angle layup on the aeroelastic characteristics of high-aspect-ratio wings.[13, 14]

The aerodynamics used in all the above investigations was based upon simple Theodorsen's strip theory. The drawback of k-type aerodynamics is that results for true aerodynamic damping at a given flight condition cannot be obtained. Also, important compressibility and finite aspect ratio effects are not accounted for. Structurally the wing was clamped at one end thus neglecting the rigid-body modes. The analyses were useful in indicating the strong influence of structural coupling, but were insufficient in terms of accuracy for practical configurations to be used for preliminary design or control synthesis.

Nonlinear aeroelastic analysis has gathered a lot of momentum in the last decade due to understanding of nonlinear dynamics as applied to complex systems and the availability of the required mathematical tools. Boyd investigated the effect of chordwise deformation and steady-state lift on the flutter of cantilevered wings.[15] He used a simplified nonlinear structural coupling between torsion and bending arising due to deformation. Theodorsen's strip theory was used for aerodynamic analysis. The studies conducted by Dugundji and his co-workers are a combination of analysis and experimental validation of the effects of structural couplings on aeroelastic instabilities for simple cantilevered laminated plate-like wings.[16, 17, 18] The studies include the effects of rigid-body motion and aerodynamic nonlinearities due to stall. Stall flutter is investigated using the ONERA stall model. Virgin and Dowell have looked into the nonlinear behavior of airfoils with control surface free-play and investigated the limit-cycle oscillations and chaotic motion of airfoils.[19, 20] On the other hand more insight into nonlinear dynamics itself using nonlinear aeroelastic behavior of an airfoil as an example

is investigated by Strganac and co-workers.[21] The importance of this work stems from the theoretical and experimental work being conducted simultaneously.

Present Work

The present work has the goal of developing a low-order ($\sim$ 500 degrees of freedom) high-fidelity aeroelastic model for preliminary design and control synthesis. In the course of the next couple of years the modeling and analysis should have achieved the following capabilities:

- Geometrically nonlinear modeling of the wing structures as beams
- Cross-sectional analysis of arbitrary, anisotropic cross sections
- Finite-state airloads modeling with compressibility
- Finite-state unsteady induced flow modeling
- ONERA stall model
- Rigid-body modes in the analysis
- Control surface aerodynamics
- Actuator dynamics
- Reduced-order control design for aircraft stabilization in the flight regime, gust load alleviation and flutter suppression.

With such a modeling capability various problems could be solved, and insights into higher-order effects gained. They include:

- Aircraft flight dynamics including aeroelastic deformation
- Aeroelastic instabilities (and the damping of various modes) of a complete aircraft
- Limit-cycle oscillations of the complete aircraft
- Parametric studies of composite wings
- Effects of steady-state lift and drag on aeroelastic characteristics
- Effect of control surface free-play
- Flight dynamics of a flexible aircraft
- Control system design and evaluation
- Aeroservoelastic tailoring of the wing/aircraft/-control system

A nonlinear aeroelastic model of a complete aircraft has been formulated. The formulation is the subject of most of the remaining paper. Preliminary results have been obtained and are presented in the final section, including trim results, flutter results for complete aircraft (flight dynamics interactions) and results which illustrate the effects of structural and aerodynamic nonlinearities. An extended analysis of the effects of nonlinearities on the flight dynamics of the complete aircraft and control system design shall be analyzed in a later paper.

Formulation

The theory is based on two separate works, viz. *i)* mixed variational formulation based on exact intrinsic equations for dynamics of moving beams;[22] and, *ii)* finite-state airloads for deformable airfoils on fixed and rotating wings.[23, 24] The former theory is a nonlinear intrinsic formulation for the dynamics of initially curved and twisted beams in a moving frame. There are no approximations to the geometry of the reference line of the deformed beam or to the orientation of the cross-sectional reference frame of the deformed beam. A compact mixed variational formulation can be derived from these equations which is well-suited for low-order beam finite element analysis based in part on Ref. 22. The latter work presents a state-space theory for the lift, drag, and all generalized forces of a deformable airfoil. Trailing edge flap deflections are included implicitly as a special case of generalized deformation. The theory allows for a thin airfoil performing arbitrary small motions with respect to a reference frame which can perform arbitrary large motions.

The formulation presented is an extension of the mixed variational formulation for dynamics of moving beams. It includes global frame motion as variable, gravitational potential and control surface dynamics. To generate the equations for this problem the only changes are the inclusion of the appropriate energies in the formulation. The equations of motion are obtained by mere application of calculus of variation.

First, a few words have to be said about the notation and the reference frames used.

There is no difference, per se, between the symbols for scalars and those used for column matrices (the elements of which are measure numbers of vectors in a certain basis). The subscript in both the cases would indicate the object or the point referred to. In the case of a column matrix, a superscript might be added to indicate with which reference frame the measure numbers are associated. The rotation matrix would be denoted by C with the superscripts indicating the two reference frames in between which it transforms; e.g., $x^a = C^{ab}x^b$.

There are various reference frames used in the formulation: 'i' is the inertial reference frame, with i_3 vertically upward (needed to define the direction of gravitational forces); 'a' is a frame attached to the aircraft, with a_2 pointing towards the nose, and a_3 pointing upward; 'b' is a series of frames attached to the undeformed beam (wing) reference line, b_1 is along the reference line; 'B' is the deformed beam reference frame; finally, 'c' and 'C' are the undeformed and deformed reference frames of the control surface at the point of attachment of the control surface to the wing.

The subscripts f, w, cs will be used to refer to properties related to the fuselage, wing, control surface respectively. The subscripts 0, b, c refer to points on the aircraft, beam reference line, control surface reference line respectively. Note that the formulation is presented here assuming just one wing for clarity. In actual implementation an user-defined number of "wings" would be allowed, thus accounting for two wings, tail wings, vertical stabilizer, canard, or any other wing-like surfaces. Similarly the various control surfaces can be attached to the various wing-like surfaces.

The variational formulation is derived from the Hamilton's principle, and can be written as,

$$\int_{t_1}^{t_2} \left(\delta(K-U) + \overline{\delta W}\right) dt = \overline{\delta \mathcal{A}}, \tag{1}$$

where K is the kinetic energy of the system, U is the potential energy of the system, $\overline{\delta W}$ represents the virtual work done on the system, $\overline{\delta \mathcal{A}}$ is the virtual action at the end of the time interval, δ is the variational operator, and t_1, t_2 specify the time interval over which the solution is required. Additional terms from the ends of the wings will be generated once the beam energies are represented as spatial integrations.

The kinetic energy of the system comes from the three subsystems which have mass, viz., fuselage, wing and control surface. The kinetic energies can be represented in the respective deformed frames as,

$$\begin{aligned}
K_f &= \tfrac{1}{2}\left(M_f {V_0^a}^T V_0^a - 2M_f \Omega_0^a \tilde{V}_0^a \xi_f + {\Omega_0^a}^T I_f \Omega_0^a\right) \\
K_w &= \tfrac{1}{2}\int_0^\ell \Big(m_w {V_b^B}^T V_b^B - 2m_w \Omega_b^B \tilde{V}_b^B \xi_w \\
&\qquad + {\Omega_b^B}^T i_w \Omega_b^B\Big)\, dx_1, \\
K_{cs} &= \tfrac{1}{2}\int_0^\ell \Big(m_{cs} {V_c^C}^T V_c^C - 2m_{cs} \Omega_c^C \tilde{V}_c^C \xi_{cs} \\
&\qquad + {\Omega_c^C}^T i_{cs} \Omega_c^C\Big)\, dx_1,
\end{aligned} \tag{2}$$

where M_f, ξ_f, I_f are, respectively, the mass, mass offset from the aircraft center of mass, and inertia matrix of the fuselage; m, ξ, i are the wing inertial properties per unit length, x_1 is the running axial coordinate along the wing and ℓ is the wing length; and column matrices V and Ω represent the total velocity and total angular velocity, respectively.

Mass also leads to gravitational potential energy. Representing it by G, the expressions for the gravitational potential energies can be written as

$$\begin{aligned}
G_f &= M_f g e_3^T C^{ia}\left(u_0^a + \xi_f\right) \\
G_w &= \int_0^\ell m_w g e_3^T C^{ia}\left(u_0^a + r_b^a + u_b^a + C^{aB}\xi_w\right) dx_1 \\
G_{cs} &= \int_0^\ell m_{cs} g e_3^T C^{ia}\left(u_0^a + r_b^a + \right. \\
&\qquad \left. u_b^a + C^{aB}\left(\xi_{b-c} + C^{BC}\xi_{cs}\right)\right) dx_1
\end{aligned} \tag{3}$$

where C denotes the rotation matrices, r denotes the position vector, ξ_{b-c} denotes the vector from point b to point c. e_i's are the unit vectors in the i^{th}-direction.

The strain energy due to elastic deformation of the wing is given by,

$$U_w = \frac{1}{2}\int_0^\ell \left\{\begin{array}{c}\gamma\\ \kappa\end{array}\right\}^T [\mathcal{S}] \left\{\begin{array}{c}\gamma\\ \kappa\end{array}\right\} dx_1 \tag{4}$$

where γ and κ are one-dimensional strain measures, and $[\mathcal{S}]$ is the 6×6 cross-sectional stiffness matrix. The stiffness matrix for arbitrary cross-section can be obtained from VABS (Variational Asymptotic Beam Sectional Analysis).[25] Note that the strain energy associated with the continuous deformation of the control surface, which is constrained to move with the wing is also a part of U_w. This contribution is obtained by calculating the cross-sectional stiffness for the complete cross section, i.e., including the control surface. Thus the cross-sectional stiffness will be a function of the control surface deflection.

The control surface is assumed to have just one degree of freedom relative to the wing. It is allowed to rotate about its reference line which is fixed in the wing. The control surface/actuator dynamics is assumed here to be due to a flexible connection. Thus, an elastic strain energy associated with this flexibility can be written as,

$$U_{cs} = \frac{1}{2}\int_0^\ell K_\vartheta(\vartheta_c - \vartheta_0)^2 dx_1 \tag{5}$$

where ϑ_0 is the control command, ϑ_c is the actual control surface deflection, and K_ϑ is the effective actuator flexibility.

Now taking the variation of individual energies, we get,

$$\begin{aligned}\delta K = \delta {V_0^a}^T P_0^a + \delta {\Omega_0^a}^T H_0^a + \int_0^\ell \Big(\delta {V_b^B}^T P_b^B + \\ \delta {\Omega_b^B}^T H_b^B + \delta {V_c^C}^T P_c^C + \delta {\Omega_c^C}^T H_c^C\Big) dx_1\end{aligned} \tag{6}$$

where the P's are the linear momenta, and H's are the angular momenta. The expressions for P and H have been derived in Ref. 26 and are given by,

$$\begin{aligned}P &= \left(\tfrac{\partial K}{\partial V}\right)^T = m\left(V - \tilde{\xi}\Omega\right) \\ H &= \left(\tfrac{\partial K}{\partial \Omega}\right)^T = i\Omega + m\tilde{\xi}V\end{aligned} \tag{7}$$

Also,

$$\delta U = \delta G + \int_0^\ell \left(\delta\gamma^T F_b^B + \delta\kappa^T M_b^B + \delta\vartheta_c M_\vartheta\right) dx_1 \tag{8}$$

where F represents the internal force, and M represents the internal moments. The expressions for F and M are obtained as

$$\begin{aligned}\left\{\begin{array}{c} F \\ M \end{array}\right\} &= \left\{\begin{array}{c} \frac{\partial U}{\partial \gamma}^T \\ \frac{\partial U}{\partial \kappa}^T \end{array}\right\} = [\,\mathcal{S}\,]\left\{\begin{array}{c} \gamma \\ \kappa \end{array}\right\} \\ M_\vartheta &= \tfrac{\partial U_c}{\partial \vartheta_c} = K_c\vartheta_c\end{aligned} \tag{9}$$

The virtual work done on the system can be written as,

$$\begin{aligned}\overline{\delta W} = \delta {u_0^a}^T f_0^a + \overline{\delta\psi_0^a}^T m_0^a + \int_0^\ell \Big(\delta {u_b^a}^T f_b^a \\ + \overline{\delta\psi_b^a}^T m_b^a + \delta\vartheta_c m_\vartheta\Big) dx_1\end{aligned} \tag{10}$$

where f, m are the external force and moment vectors. Propulsive forces and aerodynamic lift and drag are a few examples of external forces.

Now using the kinematic relationships derived in Ref. 22 and the transformed representation presented in Ref. 26, the expressions for the velocities and the generalized strains can be written as

$$\begin{aligned}V_0^a &= \dot{u}_0^a \\ \tilde{\Omega}_0^a &= -\dot{C}^{ai}{C^{ai}}^T \\ V_b^B &= C^{Ba}\left(V_0^a + \tilde{\Omega}_0^a\left(r_b^a + u_b^a\right) + \dot{u}_b^a\right) \\ \tilde{\Omega}_b^B &= -\dot{C}^{Ba}{C^{Ba}}^T + C^{Ba}\tilde{\Omega}_0^a{C^{Ba}}^T \\ V_c^C &= C^{CB}\left(V_b^B + \tilde{\Omega}_b^B\xi_{b-c}\right) \\ \tilde{\Omega}_c^C &= -\dot{C}^{CB}{C^{CB}}^T + C^{CB}\tilde{\Omega}_b^B{C^{CB}}^T \\ \gamma &= C^{Ba}\left(C^{ab}e_1 + u_b^{a\prime}\right) - e_1 \\ \kappa &= \left(C^{bB}C^{Ba\prime} - C^{ba\prime}\right)C^{ab}\end{aligned} \tag{11}$$

where $\dot{(\,)}$ denotes derivative with respect to time, and $(\,)'$ denotes derivative with respect to x_1. Before proceeding any further, it is necessary to define some rotational variables to represent the orientation of the aircraft, wing sections, and control surface. The orientation of C frame with respect to B frame can represented in terms of one angle, ϑ_c. The orientation of B frame with respect to a frame can be represented

in terms of Rodrigues parameters. Rodrigues parameters have been applied to nonlinear beam problems with success. For the orientation of the aircraft, i.e., a frame, the regular use of the Rodrigues parameters are insufficient because of a singularity at rotation of 180°. Thus, the rotation matrix will be used as rotational variable. The expression for the angular velocity will automatically constrain the six additional unknowns. Thus we have,

$$C^{ab}C^{Ba} = \frac{\left(1 - \frac{\theta_b^{aT}\theta_b^a}{4}\right) - \tilde{\theta}_b^a + \frac{\theta_b^a\theta_b^{aT}}{2}}{1 + \frac{\theta_b^{aT}\theta_b^a}{4}} \qquad (12)$$

$$C^{CB} = \begin{bmatrix} 1 & 0 & 0 \\ 0 & \cos\vartheta_c & \sin\vartheta_c \\ 0 & -\sin\vartheta_c & \cos\vartheta_c \end{bmatrix}$$

where θ_b^a are the Rodrigues parameters.

Now, the expressions for the angular velocities and moment strain can be simplified in terms of the orientation variables as

$$\Omega_b^B = C^{ba}\left(\frac{\Delta - \frac{\tilde{\theta}_b^a}{2}}{1 + \frac{\theta_b^{aT}\theta_b^a}{4}}\right)\dot{\theta}_b^a + C^{Ba}\Omega_0^a$$

$$\Omega_c^C = \dot{\vartheta}_c e_1 + C^{CB}\Omega_b^B \qquad (13)$$

$$\kappa = C^{ba}\left(\frac{\Delta - \frac{\tilde{\theta}_b^a}{2}}{1 + \frac{\theta_b^{aT}\theta_b^a}{4}}\right)\theta_b^{a\prime}$$

where Δ is the 3×3 identity matrix.

Given above are the variational forms of all the energies, and the expressions for all the variables used therein. In the mixed formulation, the variable expressions are enforced as additional constraints using Lagrange multipliers. Denoting the expressions of all the variables by $()^*$, Hamilton's equation becomes,

$$\begin{aligned}
&\int_{t_1}^{t_2}\Big\{\delta V_0^{a*T}P_0^a + \delta\Omega_0^{a*T}H_0^a + \delta u_0^{aT}f_0^a + \overline{\delta\psi}_0^{aT}m_0^a \\
&-\delta G - \delta V_0^{aT}(P_0^a - P_0^{a*}) - \delta\Omega_0^{aT}(H_0^a - H_0^{a*}) \\
&-\delta P_0^{aT}(V_0^a - V_0^{a*}) - \delta H_0^{aT}(\Omega_0^a - \Omega_0^{a*}) \\
&+\int_0^\ell\Big[\delta V_b^{B*T}P_b^B + \delta\Omega_b^{B*T}H_b^B + \delta V_c^{C*T}P_c^C \\
&+\delta\Omega_c^{C*T}H_c^C - \delta\gamma^{*T}F_b^B - \delta\kappa^{*T}M_b^B - \delta\vartheta_c U_\vartheta \\
&-\delta\vartheta_c M_\vartheta + \delta u_b^{aT}f_b^a + \overline{\delta\psi}_b^{aT}m_b^a + \delta\vartheta_c m_\vartheta \\
&+\delta\gamma^T(F_b^B - F_b^{B*}) + \delta\kappa^T(M_b^B - M_b^{B*}) \\
&-\delta V_b^{BT}(P_b^B - P_b^{B*}) - \delta\Omega_b^{BT}(H_b^B - H_b^{B*}) \\
&+\delta F_b^{BT}(\gamma - \gamma^*) + \delta M_b^{BT}(\kappa - \kappa^*) \\
&-\delta P_b^{BT}(V_b^B - V_b^{B*}) - \delta H_b^{BT}(\Omega_b^B - \Omega_b^{B*}) \\
&+\delta\vartheta_c(M_\vartheta - M_\vartheta{}^*) - \delta V_c^{CT}(P_c^C - P_c^{C*}) \\
&-\delta\Omega_c^{CT}(H_c^C - H_c^{C*}) - \delta P_c^{CT}(V_c^C - V_c^{C*}) \\
&-\delta H_c^{CT}(\Omega_c^C - \Omega_c^{C*})\Big]\,dx_1\Big\}\,dt = \overline{\delta\mathcal{A}}
\end{aligned} \qquad (14)$$

The expressions for various quantities and their variations can be substituted in the above equations to get a complete expression for the Hamilton's equation.

The external forces and moments in the above expressions are the various loads acting on the aircraft, including aerodynamic and propulsive loads. Propulsive loads will be assumed as given. The aerodynamic loads will be calculated as described in the following section.

Aerodynamic Loads

The aerodynamic loads used are as described in detail in Ref. 23. The results are presented here. The theory calculates loads on a deformable airfoil undergoing large deformation in a subsonic flow. Certain aerodynamic parameters for the particular airfoil are

required and are assumed to be known empirically or through a CFD analysis.

Let the mean chord line deformation of the airfoil cross section be described by $h(x_2, t)$ where x_2 is along the mean chord line. The frame motion along x_2, x_3-directions are, respectively, u_0, $v(x_2, t)$. Let λ denote the induced flow due to free vorticity. Let $L(x_2, t)$ denote the distribution of force perpendicular to the mean chord line. Let D be the drag on the airfoil. The integro-differential airloads equations can be converted into ordinary differential equations (ODE) through a Glauert expansion. The ODEs are in terms of the expansion coefficients which are represented by a subscript n.

$$\begin{aligned}
&\tfrac{1}{2\pi\rho}\{L_n\} = -b^2[M]\left\{\ddot{h_n} + \dot{v_n}\right\} \\
&\quad -bu_0[C]\left\{\dot{h_n} + v_n - \lambda_0\right\} - {u_0}^2[K]\{h_n\} \\
&\quad b[G]\{\dot{u_0}h_n + \bar{u_0}\zeta_n - u_0 v_n + u_0\lambda_0\} \\
&\tfrac{1}{2\pi\rho}\{D\} = -b\left\{\dot{h_n} + v_n - \lambda_0\right\}^T[S]\left\{\dot{h_n} + v_n - \lambda_0\right\} \\
&\quad +b\left\{\ddot{h_n} + \dot{v_n}\right\}^T[G]\{h_n\} \\
&\quad u_0\left\{\dot{h_n} + v_n - \lambda_0\right\}^T[K - H]\{h_n\} \\
&\quad +\{\dot{u_0}h_n + \bar{u_0}\zeta_n - u_o v_n + u_0\lambda_0\}^T[H]\{h_n\}
\end{aligned} \tag{15}$$

where ρ, b are the air density and semichord respectively. The matrices denoted by $[K]$, $[C]$, $[G]$, $[S]$, $[H]$, $[M]$ are constant matrices whose expressions are given in Ref. 23

The required airloads (viz., lift, moment about mid chord, and hinge moment) are obtained as a linear combination of L_n. The theory described so far is basically a linear, thin-airfoil theory. But the theory lends itself to corrections and modifications from experimental data. Thus, corrections such as thickness and Mach number can be incorporated very easily as described in Ref. 24

Inflow Theory The inflow is obtained through the finite-state inflow theory.[27] The inflow (λ_a) is represented in terms of N states λ_1, λ_2, ..., λ_N as

$$\lambda_a \approx \frac{1}{2}\sum_{n=1}^{N} b_n\lambda_n \tag{16}$$

where the b_n are found by least square method, and the λ_n are obtained by solving a set of N first-order differential equations[27]

$$\begin{aligned}
&\dot{\lambda}_a - \tfrac{1}{2}\dot{\lambda}_2 + \tfrac{u_T}{b}\lambda_1 = 2\dot{\bar{\Gamma}} \\
&\tfrac{1}{2n}\left(\dot{\lambda}_{n-1} - \dot{\lambda}_{n+1}\right) + \tfrac{u_T}{b}\lambda_n = \tfrac{2}{n}\dot{\bar{\Gamma}}
\end{aligned} \tag{17}$$

Where, $\bar{\Gamma}$ is the normalized circulation $\frac{\Gamma}{2\pi b}$. The expression for the normalized circulation is calculated based on the deformable airfoil model as

$$\bar{\Gamma} = \{1\}^T[C - G]\{h_n + v_n - \lambda_1\} + \frac{u_0}{b}\{1\}^T[K]\{h_n\} \tag{18}$$

Stall Model The airloads and inflow model can be modified to include the effects of dynamic stall according to the ONERA approach.

$$\begin{aligned}
&L_{T_n} = L_n + \rho u_T\Gamma_n \qquad\qquad n \geq 1 \\
&\Gamma_T = \Gamma + \Gamma_\ell
\end{aligned} \tag{19}$$

where

$$\begin{aligned}
&u_T = \sqrt{{u_0}^2 + (v_0 + \dot{h_0} - \lambda_0)^2} \\
&\ddot{\Gamma_n} + \tfrac{u_T}{b}\eta\dot{\Gamma_n} + \left(\tfrac{u_T}{b}\right)^2\omega^2\Gamma_n = \\
&\qquad -\tfrac{\omega^2{u_T}^3\Delta c_n}{b} - \omega^2 e u_T\tfrac{d}{dt}\left(u_T\Delta c_n\right)
\end{aligned} \tag{20}$$

The parameters Δc_n, η, ω^2, and e must be identified for a particular airfoil. Γ_ℓ is the correction to the circulation obtained for Δc_ℓ. To calculate the correction to Lift ($-L_0$) and drag (D) the following equations are used, which also include the effect of skin friction drag.

$$\begin{aligned}
&L_{T_0} = L_0 - \rho u_0\Gamma_\ell - c_d u_T(v_0 + \dot{h_0} - \lambda_0)\rho b \\
&D_T = D - \rho(v_0 + \dot{h_0} - \lambda_0)\Gamma_\ell + c_d u_T u_0\rho b
\end{aligned} \tag{21}$$

The airloads are inserted into the Hamilton's principle to complete the aeroelastic model.

Solution of the Aeroelastic System

Two kinds of solutions are to be found. *i)* Nonlinear steady-state solution and stability analysis about the steady state. *ii)* Nonlinear time marching solution for nonlinear dynamics of the system.

For stability analysis, the formulation is converted to it weakest form in space, while letting the time derivatives of variable remain. This is achieved by transferring the spatial derivatives of variables to the corresponding variation by integration by parts. Due to the formulation's weakest form, the simplest shape functions can be used.[22] Thus,

$$\begin{aligned}
&\delta u = \delta u_i(1-\xi) + \delta u_j \xi && u = u_i \\
&\overline{\delta\psi} = \overline{\delta\psi}_i(1-\xi) + \overline{\delta\psi}_j \xi && \theta = \theta_i \\
&\overline{\delta F} = \overline{\delta F}_i(1-\xi) + \overline{\delta F}_j \xi && F = F_i \\
&\overline{\delta M} = \overline{\delta M}_i(1-\xi) + \overline{\delta M}_j \xi && M = M_i \\
&\overline{\delta P} = \overline{\delta P}_i && P = P_i \\
&\overline{\delta H} = \overline{\delta H}_i && H = H_i
\end{aligned} \tag{22}$$

With these shape functions, the spatial integration in Eq. (14) can be performed explicitly to give a set of nonlinear equations as described in Ref. 28. These equations can be separated into structural (F_S) and aerodynamic (F_L) terms and written as

$$F_S(X, \dot{X}) - F_L(X, Y, \dot{X}) = 0 \tag{23}$$

where X is the column matrix of structural variables and Y is a column matrix of inflow states. Similarly we can separate the inflow equations into an inflow component (F_I) and a downwash component (F_W) as

$$-F_W(\dot{X}) + F_I(Y, \dot{Y}) = 0 \tag{24}$$

The solutions of interest for the two coupled sets of equations (Eqs. 23 and 24) can be expressed in the form

$$\begin{Bmatrix} X \\ Y \end{Bmatrix} = \begin{Bmatrix} \bar{X} \\ \bar{Y} \end{Bmatrix} + \begin{Bmatrix} \check{X}(t) \\ \check{Y}(t) \end{Bmatrix} \tag{25}$$

where $\bar{(\ )}$ denotes steady-state solution and $\check{(\ )}$ denotes the small perturbation on it.

For the steady-state solution one gets $\bar{Y}$ identically equal to zero (from Eq. 24). Thus, one has to solve a set of nonlinear equations given by

$$F_S(\bar{X}, 0) - F_L(\bar{X}, 0, 0) = 0 \tag{26}$$

The Jacobian matrix of the above set of nonlinear equations can be obtained analytically and is found to be very sparse.[28] The steady-state solution can be found very efficiently using Newton-Raphson method. Once a steady-state solution is obtained, stability analysis about the steady state is conducted.

By perturbing Eqs. (23) and (24) about the calculated steady state using Eq. (25), the transient solution is obtained from

$$\begin{aligned}
&\begin{bmatrix} \frac{\partial F_S}{\partial X} - \frac{\partial F_L}{\partial X} & -\frac{\partial F_L}{\partial Y} \\ 0 & \frac{\partial F_I}{\partial Y} \end{bmatrix}_{\substack{X=\bar{X} \\ Y=0}} \begin{Bmatrix} \check{X} \\ \check{Y} \end{Bmatrix} + \\
&\begin{bmatrix} \frac{\partial F_S}{\partial \dot{X}} - \frac{\partial F_L}{\partial \dot{X}} & 0 \\ -\frac{\partial F_W}{\partial \dot{X}} & \frac{\partial F_I}{\partial \dot{Y}} \end{bmatrix}_{\substack{X=\bar{X} \\ Y=0}} \begin{Bmatrix} \dot{\check{X}} \\ \dot{\check{Y}} \end{Bmatrix} = \begin{Bmatrix} 0 \\ 0 \end{Bmatrix}
\end{aligned} \tag{27}$$

Now assuming the dynamic modes to be of the form e^{st}, the above equations can be solved as an eigenvalue problem to get the modal damping, frequency and mode shape of the various modes. The stability condition of the aeroelastic system at various operating conditions (steady states) is thus obtained.

Nonlinear dynamics of aeroelastic system

To investigate the nonlinear dynamics of the aircraft a time history of aircraft motion and deformation has to be obtained. To get such a solution space-time finite elements are used. This requires that the formulation be converted into its weakest form in space as well as time. Thus, the spatial and temporal derivatives are transferred to the variations. To get the space-time finite elements the following shape

functions have to be used?[29]

$$
\begin{aligned}
\delta u &= \delta u_i(1-\xi)(1-\tau) + \delta u_j \xi(1-\tau) \\
&\quad + \delta u_k \xi\tau + \delta u_l(1-\xi)\tau && u = u_i \\
\overline{\delta\psi} &= \overline{\delta\psi}_i(1-\xi)(1-\tau) + \overline{\delta\psi}_j\xi(1-\tau) \\
&\quad + \overline{\delta\psi}_k\xi\tau + \overline{\delta\psi}_l(1-\xi)\tau && \theta = \theta_i \\
\overline{\delta F} &= \overline{\delta F}_i(1-\xi) + \overline{\delta F}_j\xi && F = F_i \\
\overline{\delta M} &= \overline{\delta M}_i(1-\xi) + \overline{\delta M}_j\xi && M = M_i \\
\overline{\delta P} &= \overline{\delta P}_i(1-\tau) + \overline{\delta P}_j\tau && P = P_i \\
\overline{\delta H} &= \overline{\delta H}_i(1-\tau) + \overline{\delta H}_j\tau && H = H_i
\end{aligned}
\tag{28}
$$

where τ and ξ are dimensionless elemental temporal and spatial co-ordinates. With these shape function the equations (Eqs 23 and 24) take the form,

$$
\begin{aligned}
&F_S(X_i, X, X_f) - F_L(X_i, X, X_f, Y) = 0 \\
&-F_W(X_i, X, X_f) + F_I(Y_i, Y, Y_f) = 0
\end{aligned}
\tag{29}
$$

where subscripts i, f, represent the variable values at the initial and final time. If the initial conditions and time interval are specified, the variable values during the time interval, and the final condition is obtained by solving the set of nonlinear equations. Thus, the solution history is obtained and the nonlinear dynamic behavior can be interpreted.

Preliminary Results

Flutter and divergence results have been obtained for a metallic wing of Ref. 30, and compared with published results (available for the linear case). The results obtained indicate that the steady state solution and the eigenvalues can be computed efficiently and are accurate. The Goland metallic wing was used as a test case since it is based on a real wing and thus gives a realistic idea of the effect of non-linearities in wings. Aeroelastic tailoring of composite box beam "wing" was conducted in an earlier paper[13] and will not be repeated here.

Test Case Data

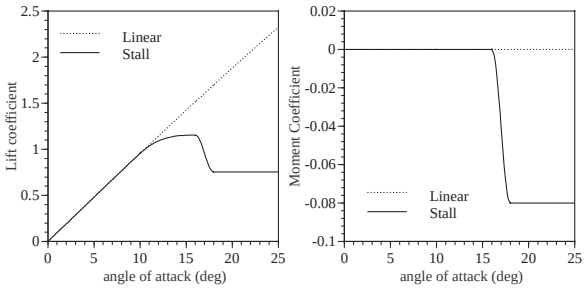

Figure 1: Linear and stall data for c_ℓ and c_m

The Goland wing data is given in Ref. 30. Other aircraft data (tail data, fuselage data) was created and added to the wing model to get a complete aircraft model as described below:

Wing half span = 20 ft
Wing chord = 6 ft
Mass per unit length = 0.746 slugs per ft
Radius of gyration of wing about mass center = 25 % of chord
Spanwise elastic axis of wing = 33 % of chord (from l.e.)
Center of gravity of wing = 43 % of chord (from l.e.)
Bending rigidity (EI_b) = 23.65×10^6 lb ft^2
Torsional rigidity (GJ) = 2.39×10^6 lb ft^2
Tail position = 10 ft behind wing elastic axis
Tail half span = 4 ft
Tail chord = 3 ft
Control surface = 50 % of chord
Mass per unit length (tail) = 0.373 slugs per ft
Radius of gyration of the tail = 25 % of chord
Center of gravity of tail = 50 % of chord (from l.e.)
Mass of fuselage = 149.2 slugs
Radius of gyration of fuselage = 6 ft
Mass offset = 1 ft in ahead of wing elastic axis

The aerodynamic data for the airfoil is obtained by curve-fitting the c_ℓ and c_m data given in Ref. 31. Fig. 1 shows the plot of the assumed linear and stall data. The coefficients for the dynamic stall model,

	Flutter Vel. (fps)	Flutter Freq. (rad/s)
Present Analysis	445	70.2
Exact Solution	450	70.7
Galerkin Solution	445	70.7

Table 1: Comparison of flutter results for Goland wing

i.e. η, ω and e for a symmetrical airfoil are given as a function of Δc_ℓ in Ref. 32 as,

$$\begin{aligned} \eta &= 0.25 + 0.10(\Delta c_\ell)^2 \\ \omega &= 0.20 + 0.10(\Delta c_\ell)^2 \\ e &= 3.3 - 0.3(\Delta c_\ell)^2 \end{aligned} \tag{30}$$

As shown in Table 1, the current analysis gives the flutter speed and flutter frequency results to within 1 % of the "exact" linear flutter speed of the cantilevered wing.

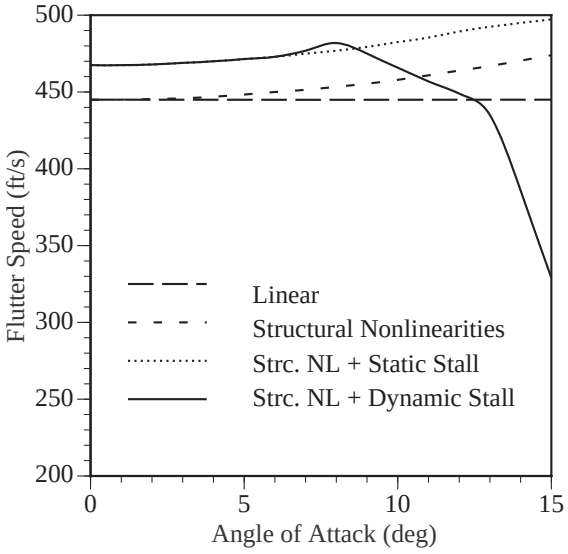

Figure 2: Variation of flutter speed with angle of attack

Effect of Nonlinearities on Flutter

Structural as well as aerodynamic nonlinearities are known to affect flutter. One of the goals of this research is to be able to determine up front those cases for which nonlinear models are essential for accuracy. As a first step towards that goal, flutter analysis is conducted on the Goland cantilevered wing. The gravitational forces and skin friction drag are neglected in these results. Fig. 2 shows the variation of the flutter speed with increasing angle of attack. The results show the effect of structural nonlinearities, nonlinear static experimental aerodynamic data, and, dynamic stall model on the flutter speed.

As the angle of attack is increased, the aerodynamic load on the wing increases and so do the bending and torsional displacements. The flutter speed is seen to increase due to geometric stiffening. If experimental static aerodynamic data are included in the analysis, then the flutter speed increases even more due to the lower lift-curve slope in the experimental data (i.e., 5.5 as compared to the theoretical value of 2π). Again there is a slight increase in flutter speed with angle of attack due to geometric stiffening. The results including dynamic stall model are markedly different from those without. This is due to coupling between the structural states and the stall states. The stall delay frequency of around 25 rad/sec interacts with the first two structural modes, leads to additional coupling and coalesence, and change in flutter mode. The flutter mode frequency shifts from around 70 rad/sec at 7° to 55 rad/sec at 12°. Also as the angle of attack is increased wing stall occurs at lower speeds and thus the lower stall flutter speed.

The effects of structural nonlinearities seem to be small in the above test case which is a low aspect ratio conventional wing. The effects would be considerably higher for a flexible high aspect ratio wings used in UAVs. More work on different models will be presented in a later paper.

Effect of Rigid-Body Motion

To quantify the effects of rigid body motion and flight dynamic interactions, the Goland wing model was extended *ad hoc* to create an aircraft model. Fig. 3 shows the root loci plot of some eigenvalues of the system with velocity. There are two sets of curves, one for the cantilevered wing and another for the complete aircraft. Again for the test case one does not see much differece between the two results, except that the phugoid mode is captured if the analysis includes rigid-body modes. One can expect more flight dynamic interactions for a flexible wing where

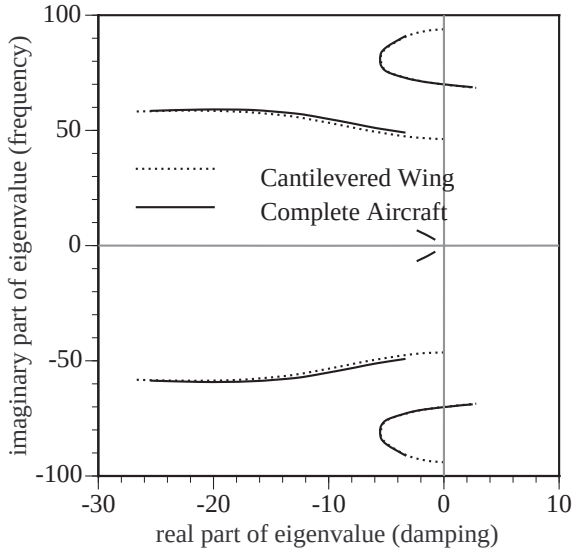

Figure 3: Root loci plot of the aeroelastic aircraft model

the structural frequencies will be lower and closer to the rigid body frequencies.[16]

Conclusions

An aeroelastic analysis tool has been developed with a capability to model the complete aircraft as a set of beams. A geometrically exact mixed formulation for the structural dynamics analysis is coupled to a finite-state airloads model which includes both an inflow model and the ONERA dynamic stall model. Validation studies were conducted on the Goland metallic wing and for a complete aircraft model extrapolated from it. The results indicate the necessity of including higher-order nonlinear effects for accurate aeroelastic analysis.

The aeroelasticity and flight dynamics code will be used to investigate in depth the effects of nonlinearities on aeroelastic behavior by studying various kinds of aircraft. Results from that study will be presented in a later paper.

References

[1] Anonymous, , "New World Vistas: Air and Space Power for the 21st Century.," USAF Scientific Advisory Board Report, Summary Volume., 1995.

[2] Howard, R. M., Bray, R. M., and Lyons, D. F., "Flying-Qualities Analysis of an Unmanned Air Vehicle," *Journal of Aircraft*, Vol. 33, No. 2, 1996, pp. 331 – 336.

[3] Ozimina, C. D., Tayman, S. K., and Chaplin, H. E., "Flight Control System Desigh for a Small Unmanned Aircraft," In *Proceedings of the american Control Conference*, Seattle, Washington, June 1995.

[4] Guruswamy, G. P. and Byun, C., "Direct Coupling of Euler Flow Equations with Plate Finite Element Structures," *AIAA Journal*, Vol. 33, No. 2, Feb. 1995, pp. 375 – 377.

[5] Shirk, M. H., Hertz, T. J., and Weisshaar, T. A., "Aeroelastic Tailoring – Theory, Practice, and Promise," *Journal of Aircraft*, Vol. 23, No. 1, Jan. 1986, pp. 6 – 18.

[6] Weisshaar, T. A., "Aeroelastic Tailoring of Forward Swept Composite Wings," *Journal of Aircraft*, Vol. 18, No. 8, Aug. 1981, pp. 669 – 676.

[7] Librescu, L. and Song, O., "On the Static Aeroelastic Tailoring of Composite Aircraft Swept Wings Modelled as Thin-Walled Beam Structures," *Composites Engineering*, Vol. 2, No. 5-7, 1992, pp. 497 – 512.

[8] Librescu, L., Meirovitch, L., and Song, O., "Refined Structural Modeling for Enhancing Vibrational and Aeroelastic Characteristics of Composite Aircraft Wing," *Recherche Aerospatiale*, 1996, pp. 23 – 35.

[9] vanSchoor, M. C. and vonFlotow, A. H., "Aeroelastic Characteristics of a Highly Flexible Aircraft," *Journal of Aircraft*, Vol. 27, No. 10, Oct. 1990, pp. 901 – 908.

[10] Butler, R. and Banerjee, J. R., "Optimum Design of Bending-Torsion Coupled Beams with Frequency or Aeroelastic Constraints," *Computers & Structures*, Vol. 60, No. 5, 1996, pp. 715 – 724.

[11] Lillico, M., Butler, R., Guo, S., and Banerjee, J. R., "Aeroelastic Optimization of Composite Wings Using the Dynamic Stiffness Method," *Aeronautical Journal*, Vol. 101, 1997, pp. 77 –86.

[12] Chattopadhyay, A., Zhang, S, and Jha, R., "Structural and Aeroelastic Analysis of Composite Wing Box Sections Using Higher-Order Laminate Theory," In *Proceedings of the 37th Structures, Structural Dynamics, and Materials Conference*, Salt Lake City, Utah, April 1996.

[13] Cesnik, C. E. S., Hodges, D. H., and Patil, M. J., "Aeroelastic Analysis of Composite Wings," In *Proceedings of the 37th Structures, Structural Dynamics, and Materials Conference*, Salt Lake City, Utah, April 18 – 19, 1996.

[14] Patil, M. J., "Aeroelastic Tailoring of Composite Box Beams," In *Proceedings of the 35th Aerospace Sciences Meeting and Exhibit*, Reno, Nevada, Jan. 1997.

[15] Boyd, N., *Effect of Chordwise Deformation and Steady-State Lift on Flutter of a Cantilevered Wing*, Ph.D. Thesis, Stanford U., California, 1977.

[16] Chen, G-S and Dugundji, J., "Experimental Aeroelastic Behavior of Forward-Swept Graphite / Epoxy Wings with Rigid-Body Freedom," *Journal of Aircraft*, Vol. 24, No. 7, July 1987, pp. 454 – 462.

[17] Dunn, P. and Dugundji, J., "Nonlinear Stall Flutter and Divergence Analysis of Cantilevered Graphite/Epoxy Wings," *AIAA Journal*, Vol. 30, No. 1, Jan. 1992, pp. 153 – 162.

[18] Dugundji, J., "Nonlinear Problems of Aeroelasticity," In Atluri, S. N., editor, *Computational Nonlinear Mechanics in Aerospace Engineering*, chapter 3. AIAA, Washington, DC, 1992.

[19] Virgin, L. N. and Dowell, E. H., "Nonlinear Aeroelasticity and Chaos," In Atluri, S. N., editor, *Computational Nonlinear Mechanics in Aerospace Engineering*, chapter 15. AIAA, Washington, DC, 1992.

[20] Conner, M. D., Virgin, L. N., and Dowell, E. H., "Accurate Numerical-Integration of State-Space Models for Aeroelastic Systems with Free Play," *AIAA Journal*, Vol. 34, No. 10, 1996, pp. 2202 – 2205.

[21] Gilliatt, H. C., Strganac, T. W., and Kurdila, A. J., "Nonlinear Aeroelastic Response of an Airfoil," In *Proceedings of the 35th Aerospace Sciences Meeting and Exhibit*, Reno, Nevada, Jan. 1997.

[22] Hodges, D. H., "A Mixed Variational Formulation Based on Exact Intrinsic Equations for Dynamics of Moving Beams," *International Journal of Solids and Structures*, Vol. 26, No. 11, 1990, pp. 1253 – 1273.

[23] Peters, D. A. and Johnson, M. J., "Finite-State Airloads for Deformable Airfoils on Fixed and Rotating Wings," In *Symposium on Aeroelasticity and Fluid/Structure Interaction, Proceedings of the Winter Annual Meeting*. ASME, November 6 – 11, 1994.

[24] Peters, D. A., Barwey, D., and Johnson, M. J., "Finite-State Airloads Modeling with Compressibility and Unsteady Free-Stream," In *Proceedings of the Sixth International Workshop on Dynamics and Aeroelastic Stability Modeling of Rotorcraft Systems*, November 8 – 10, 1995.

[25] Cesnik, C. E. S. and Hodges, D. H., "VABS: A New Concept for Composite Rotor Blade Cross-Sectional Modeling," *Journal of the American Helicopter Society*, Vol. 42, No. 1, January 1997, pp. 27 – 38.

[26] Shang, X. and Hodges, D. H., "Aeroelastic Stability of Composite Rotor Blades in Hover," In *Proceedings of the 36th Structures, Structural Dynamics and Materials Conference*, New Orleans, Louisiana, April 10 – 12, 1995, pp. 2602 – 2610, AIAA Paper 95-1453.

[27] Peters, D. A., Karunamoorthy, S., and Cao, W.-M., "Finite State Induced Flow Models; Part I : Two-Dimensional Thin Airfoil," *Journal of Aircraft*, Vol. 32, No. 2, Mar.-Apr. 1995, pp. 313 – 322.

[28] Hodges, D. H., Shang, X., and Cesnik, C. E. S., "Finite Element Solution of Nonlinear Intrinsic Equations for Curved Composite Beams," *Journal of the American Helicopter Society*, Vol. 41, No. 4, Oct. 1996, pp. 313 – 321.

[29] Atilgan, A R., Hodges, D. H., Ozbek, A. M., and Zhou, W., "Space-Time Mixed Finite Elements for Rods," *Journal of Sound and Vibration*, Vol. 192, No. 3, May 9 1996, pp. 731 – 739.

[30] Goland, M., "The Flutter of a Uniform Cantilever Wing," *Journal of Applied Mechanics*, Vol. 12, No. 4, December 1945, pp. A197 – A208.

[31] McAlister, K. W., Lambert, O., and Petot, D., "Application of the ONERA Model of Dynamic Stall," Technical report, NASA-TP-2399, Nov. 1984.

[32] Peters, D. A., Barwey, D., and Su, A., "An Integrated Airloads-Inflow Model for Use in Rotor Aeroelasticity and Control Analysis," *Mathematical and Computational Modelling*, Vol. 19, No. 3/4, 1994, pp. 109 – 123.